A sensitivity-based analysis for managing storage capacity of a small agricultural reservoir under drying climate

Daeha Kim[a,*], Hyung-Il Eum[a,1], Jagath J. Kaluarachchi[b], Jong Ahn Chun[a]

[a] *Climate Services and Research Department, APEC Climate Center, Busan, 48058, South Korea*
[b] *College of Engineering, Utah State University, Logan, Utah, 84322-4100, USA*

ARTICLE INFO

ABSTRACT

Reservoirs have played a vital role in sustaining agricultural production and human livelihood with changing environments and demands. While expanding the storage capacity of a reservoir is deemed a robust structural adaptation that improves water allocation, few studies have discussed the sensitivity of this approach to climatic stresses. In this study, we investigated the effectiveness of building and upsizing reservoirs on addressing water scarcity under climate change in a simple reservoir system in South Korea. We employed a sensitivity-based framework that combines a stochastic system analysis and climate projections, and assessed the response of mean water scarcity to climatic stresses. Results showed that building or upsizing a reservoir made system performance more responsive to climatic stresses. Although additional reservoir capacity can help reducing water scarcity, the effectiveness of such an approach is expected to diminish rapidly when climate becomes drier. If existing climate changes towards drier conditions, performance achieved through additional storage capacity decreases more rapidly, resulting in lager performance loss than before making structural measures. This study suggests that the direction of climate change and operational upgrades should be considered to reduce potential shortcomings associated with the structural adaptation strategies for a simple reservoir system.

1. Introduction

By intervening in natural river flows, reservoirs have provided additional water availability and benefits to humans (Biemans et al., 2011). More than half of river systems in the world are regulated by reservoirs to sustain irrigation and economic activities (Nilsson et al., 2005). However, climatic change driven by anthropogenic greenhouse gas (GHG) emissions could pose challenges to reservoir systems (Steinschneider and Brown, 2012). Nonstationary climate may alter probabilistic behaviors of hydrologic processes; thereby, undermines heuristic operation policies by which most reservoirs and river systems have been traditionally managed (Whateley et al., 2014; Georgakakos et al., 2012).

Among various adaptation strategies to address climate change for agricultural systems, upsizing or building reservoirs is deemed a robust strategy that can reduce the spatiotemporal variation of surface water availability (Iglesias and Garrote, 2015; Hallegatte, 2009). Although a structural intervention in a natural river system may lead to environmental adverse effects (Poff and Olden, 2017; Poff and Schmidt, 2016; Ngigi, 2003), the human-made water holding capacity and allocation inarguably plays a crucial role in satisfying agricultural demands (Ehsani et al., 2017; Khagram, 2004). In particular, micro-storage facilities (e.g., small reservoirs, farm ponds, and underground tanks) require relatively low effort for construction and maintenance, and thus seem more economically viable than large-scale water infrastructure (Wisser et al., 2010). In India, for example, small reservoirs have rapidly spread over agricultural regions during the past two decades, approximately supplying 20% of the total irrigation (Downing et al., 2006; Li and Gowing, 2005). Wisser et al. (2010) highlighted that construction of small reservoirs can increase the global cereal production by 35%. Hence, structural investments such as building small reservoirs appear to be an attractive solution to reduce climate change risks in low-yield regions under drought-prone environments.

Nonetheless, an efficient adaptation mechanism is to reduce sensitivity (or improve robustness) of agricultural systems to climate change stresses (Wilby and Dessai, 2010; Adgar et al., 2005). In practice, policymakers may seek "low-regret" options that enable a given system to withstand a certain level of climatic stresses without substantial losses rather than selecting options that maximizes benefits (Weaver et al., 2013). In this regard, questions arise as to whether building or upsizing

reservoirs can lower responsiveness of a water supply system to climatic stresses, and to whether a structural investment can be a low-regret adaptation policy. Those questions seem to have been overlooked in many studies that explored efficiency improvements for existing large and complex reservoir systems under changing socioeconomic and climatic constraints (e.g., Georgakakos et al., 2012; Eum and Simonovic, 2010).

Furthermore, many climate change impact assessments have depended on few projections of general circulation models (GCM). GCM-based top-down assessments (i.e., from climate projections to system analysis) have the difficulty to provide the information necessary for decision-making such as visualization of climatic risks and sensitivity of system performance (Brown and Wilby, 2012). Although novel decision-centric approaches have emerged (e.g., Steinschneider et al., 2015; Whateley et al., 2014; Turner et al., 2014), few studies have focused on responses of micro-storage facilities to climate change. The purpose of this study is therefore to investigate the effectiveness of structural improvements under climate change via a case study for a small reservoir that provides agricultural water in a region of South Korea. To understand sensitivity of the reservoir performance to climate change, we employed a decision-centric method that combines a stochastic system analysis and GCM projections. The response functions were developed between a pre-defined water scarcity metric and a set of climatic variables. Climate change impacts were assessed by overlaying numerous GCM projections on the response functions.

2. Description of study area and data

2.1. Yangak agricultural reservoir

The study area is the Yangak reservoir located in central South Korea (Fig. 1). The relatively small reservoir system is designed to supply irrigation water to rice-planting lands at the downstream area. We conceptualized the agricultural reservoir system as a simple node-and-link model with single supply and demand nodes representing the watershed and the agricultural sector, respectively. The reservoir interplays between the supply and demand nodes by regulating natural river flows. The watershed has an area of $13.4\,km^2$, and the rice-planting lands account for 3.75 ha. The reservoir has a storage capacity of $2.3\,Mm^3$ with a dead storage of $0.09\,Mm^3$. To reduce climatic risk, the Korea Rural Community Corporation recently expanded the storage capacity of the reservoir to $3.3\,Mm^3$.

Water management in the study area is affected by typical monsoonal climate that brings wet summer seasons. Approximately, 60–70% of precipitation falls from late June to September, generating high streamflow. Because the streamflow continuously reduces after a rainy season, water stored in the reservoir during a dry season is essential to meet the large demand for rice transplanting in May and June. Due to low winter precipitation, snowmelt has minimal contribution to water supply in the spring season (Bae et al., 2008).

2.2. Climate data

To simulate reservoir inflows and agricultural water demand, we used gridded daily precipitation, and maximum and minimum temperatures for 1976–2015 at 3-km resolution produced by a geospatial interpolation technique (Daly et al., 2008) with 60 automated synoptic observing stations (ASOS) of the Korea Meteorological Administration (Eum, 2015). Jung and Eum (Jung and Eum, 2015) validated the performance of the gridded daily data set using separate observations at 243 automated weather stations across South Korea.

We averaged grid data within the boundary of the watershed and at the rice-planting pixels respectively. Long-term climate of the reservoir system (i.e., mean annual precipitation and temperatures) was represented by averages between the watershed and the agricultural sector. The mean annual precipitation and temperature were 1563 mm and 11.9 °C during 1976–1995. Both values increased to 1650 mm and 12.2 °C during 1996–2015, indicating that atmospheric water supply (i.e., precipitation) and evaporative demand (i.e., potential evapotranspiration; PET) seem to rise over time.

3. Methodology

3.1. Proposed framework

We employed the bottom-up decision scaling framework (Brown et al., 2012) that combines a system sensitivity analysis with climate projections. While a typical scenario-based impact assessment investigates changes in model outputs forced by downscaled GCMs (e.g., Raje and Mujumdar, 2010; Vano et al., 2010), the decision scaling uses the climate response function (CRF) developed by system models and stochastically generated climatic inputs. The impacts of climate change can be assessed using the sensitivity of the performance indicator to changing climates via plotting multiple GCM projections on the CRF. This sensitivity-based bottom-up assessment (i.e., from system analyses to climate projections) allows policymakers to integrate system responses to different climate conditions for a given decision criterion. Because numerous GCM projections can be assessed together using the CRF, the decision-scaling framework makes it possible to avoid risky adaptation policies from a small collection of climate change
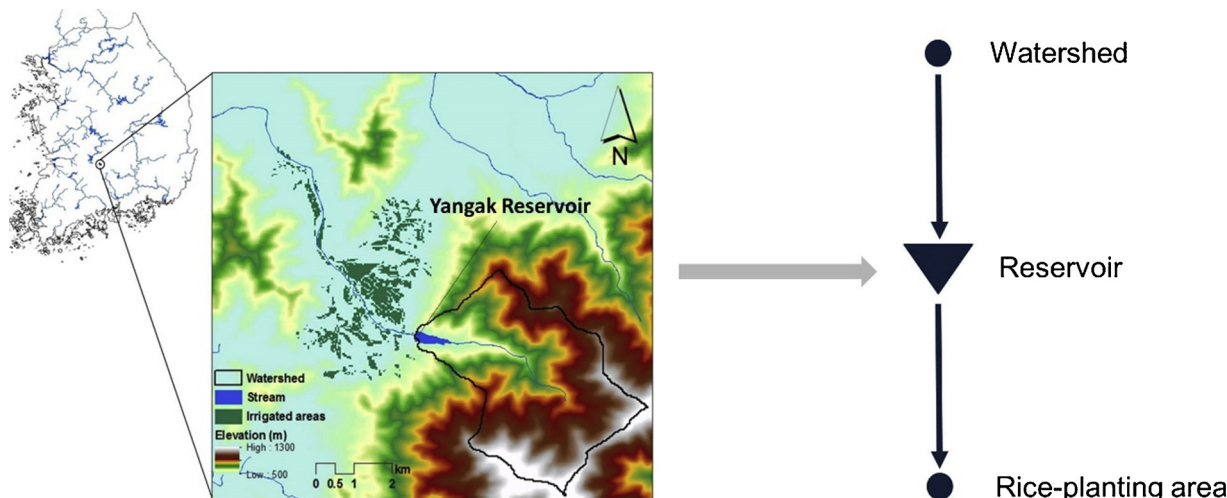

Fig. 1. Physical layout of the study area and the node-and-link conceptualization.

projections with substantial uncertainty (Brown et al., 2012).

In this work, we assessed climate change impacts on water scarcity in the agricultural demand sector. First, we defined the water scarcity index using monthly estimates of water supply and demand as:

$$I_t = (S_t - D_t)/D_t \tag{1}$$

where, I_t, S_t, and D_t are water scarcity index (unitless), water supply (Mm^3), and water demand (Mm^3) at month t, respectively. It represents the magnitude of water shortage relative to water demand.

The primary focus of this study is the magnitude of water scarcity in the reservoir system under various climatic stresses. Since climate change is typically represented by climatological changes for a decade or longer period (IPCC, 2007), we defined the mean water scarcity, which is equivalent to the definition of vulnerability in Hashimoto et al. (1982), for a bi-decadal period (ν) using the average of negative I_t values:

$$\nu = |E[I_t \mid I_t < 0]| \tag{2}$$

We analyzed responses of mean water scarcity to bi-decadal mean precipitation and temperature (hereafter referred to as P_{avg} and T_{avg}, respectively). To develop the relationship of ν to P_{avg} and T_{avg}, stochastic generations are essential because only one set of mean precipitation and temperature can be achieved from 20-year-long climatic data. The following section describes the stochastic weather generations applied.

3.2. Stochastic generation of climate data

Precipitation and temperatures should be major drivers of natural inflows and agricultural water demand. To have extensive climatic data required for developing the CRFs, we used a Markov chain model and the first-order vector autoregressive (VAR1) model formulated by Wilks (1999), which have been widely used in many studies (e.g., Keller et al., 2015; Srikanthan and Pegram, 2009). We briefly described the stochastic generations here, and more details about the models are found in Wilks (1999).

The precipitation generator uses the Markov chain and the mixed exponential distribution for precipitation occurrence and amount processes, respectively. Using the precipitation datasets for 1976–2015, we estimated the transition probabilities of the Markov chain and the parameters of the mixed exponential distribution for each month from January to December. A pair of 10,000-year-long daily precipitation time series was generated for the watershed and demand nodes using spatially correlated random numbers. For temperature generation, the parameter matrices of the VAR1 model were analytically estimated with the vector of temperature data sets standardized by a single wave cosine function. Using the parameter matrices, daily maximum and minimum temperatures were generated for the watershed and demand nodes for the same length of stochastic precipitation.

While the skewed distribution of the precipitation model could provide a relatively wide range of bi-decadal averages from 10,000-year-long generations, the symmetric Gaussian distribution of the VAR1 model produced a minimal variation in bi-decadal mean temperatures. To extend the narrow range of the mean temperatures, we did a simple post-processing for the stochastic temperatures. The 10,000-year-long daily temperatures were divided into 120,000 sets for each year and each month from January to December (i.e., 10,000 sets for each month). We sorted the 10,000 daily temperature sets of each month by their averages in ascending order (i.e., sorting from the coldest to the warmest years). Then, the twelve sets with the same order were recombined to represent the annual variations from January to December. This reordering allowed to have an extended range of bi-decadal mean temperatures from the coldest to the warmest bi-decadal periods. Even after post processing, stochastic daily temperatures are still plausible values reproducing the averages and variances of the daily observations.

3.3. Simulation of reservoir inflows

The conceptual streamflow model GR4J (Perrin et al., 2003) was used to simulate daily inflows to the Yangak reservoir using the stochastic precipitation and temperatures. GR4J conceptualizes the watershed response to atmospheric drivers (daily precipitation and PET) with four free parameters that represent soil water storage, groundwater exchange, routing storage, and the basetime of unit hydrograph. GR4J is widely used under diverse hydro-climatic conditions based on its parsimonious structure and robust predictions (Zhang et al., 2015). Computational details for streamflow simulations are available in Perrin et al. (2003).

Since no inflow records were available for the Yangak reservoir, we applied an approach for ungauged basins. Kim et al. (2017) evaluated the predictive performance of a parameter regionalization approach in comparison to the calibration against a regional flow duration curve (FDC), concluding that transferring parameter sets from nearby gauged watersheds is preferable in South Korea. The median Nash Sutcliffe Efficiency of the proximity-based parameter regionalization was 0.65 with an interquartile range of 0.27. To simulate the reservoir inflows, we used the parameter sets of the five gauged watersheds in Kim et al. (2017) in proximity to the Yangak Reservoir. We took the averages of five daily runoff time series simulated using the stochastic inputs and the transferred parameters, and the monthly inflows were gained by aggregating the daily flows. In the runoff simulations, the temperature-based model proposed by Oudin et al. (2005) was used to estimate PET.

3.4. Estimation of water demands

The water demand at rice-planting lands was estimated using the guideline of the Food and Agriculture Organization (FAO) of the United Nations (Allen et al., 1998). The crop water requirements were calculated using the FAO Penman-Monteith equation on a daily basis as:

$$ET_o = \frac{0.408\Delta(R_n - G) + \gamma \frac{900}{T+273} u_2 (e_s - e_a)}{\Delta + \gamma(1 + 0.34 u_2)} \tag{3a}$$

$$ET_c = K_c \times ET_o \tag{3b}$$

where ET_o is reference ET ($mm\ d^{-1}$), R_n is net radiation at the crop surface ($MJ\ m^{-2}\ d^{-1}$), G is soil heat flux ($MJ\ m^{-2}\ d^{-1}$), T is mean air temperature at 2 m height (°C), u_2 is wind speed at 2 m height ($m\ s^{-1}$), e_s and e_a are saturation and actual vapor pressures (kPa), respectively, Δ is the slope of vapor pressure curve ($kPa\ °C^{-1}$), γ is the psychrometric constant ($kPa\ °C^{-1}$), K_c is the crop coefficient (unitless), and ET_c is the crop ET ($mm\ d^{-1}$).

For ET_c estimation using the stochastically generated temperatures, we used the average u_2 values on each day of year obtained from observations at the nearest weather station to the Yangak reservoir. e_a was estimated using the minimum temperature as the recommendation of Allen et al. (1998). Crop coefficient K_c was from an experimental study conducted by Yoo et al. (2006) at an interval of 10 days for South Korea.

Along with ET_c, we considered the water requirement for preparing and transplanting rice seedlings, which is a common rice-cropping practice in South Korea. Typically, 140 mm of water is needed to prepare rice seedbeds for 4 days (i.e., 35 mm d^{-1}) over 1/20 of the planting area. For the next 30 days, ET_c of seedlings becomes the water requirement over the area of rice seedbeds. The rice seedlings are transplanted for the following 20 days, requiring additional 14 mm of irrigation per day over the planting area. The total growing period was assumed as 150 days from a typical beginning date of preparing rice seedbeds (April 15th). The diversion efficiency was assumed to be 0.7 between the reservoir and the rice-planting lands (Cho et al., 2016).

In addition, we considered the environmental water demand. In South Korea, it is recommended that streamflow should be maintained above the standard drought flow, which could be estimated as the flow
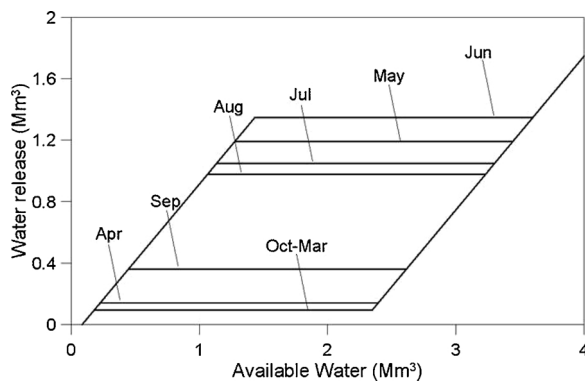
Fig. 2. The standard operating rules for the reservoir capacity of 2.3 Mm^3.

at the exceedance probability of 355/365 from the period-of-record FDC. We simulated streamflow in the watershed using GR4J with observed precipitation and temperatures for 1976–2015, and determined the environmental demand to be 0.035 m^3 s^{-1}.

3.5. Reservoir operation

More than 17,000 small agricultural reservoirs are spread over South Korea; hence, it has been difficult to operationally monitor reservoir inflows and outflows. No outflow records were available for the Yangak Reservoir too. Thus, we hypothesized that the standard operating policy (SOP; Loucks and van Beek, 2016; Stedinger, 1984; Maass et al., 1962) was applied to the reservoir system because it is the optimal operating policy when the loss function is linear (Hashimoto et al., 1982). The SOP, therefore, may be the best option for this case study to minimize water scarcity at a single demand sector. A hedging rule, which saves water for future benefits even under unsatisfactory water availability (e.g., Eum et al., 2011), is unlikely activated, because future water supply may not compensate early crop failures or yield losses from water stress.

The SOP for the Yangak reservoir (Fig. 2) was set by the average demands for the twelve months (i.e., fixed demand targets for each

month) obtained from the monthly demand estimates for 1976–2015. The expected water availability at the beginning of a given month was calculated by summing water availability at the end of the previous month and the expected inflow minus evaporation loss in the current month. In other words, it was assumed that the water manager supplies water to the demand sector based on averages of historical inflows and demands. This management may produce operational water shortage, when the expected water availability (or demand) is less (or greater) than actual.

3.6. Developing climate response functions

We produced a 10,000-year-long time series of I_t using the monthly estimates of water supply (i.e., reservoir outflows) and demands. Subsequently, the mean water scarcity (ν) was quantified for each 20-year time slice. After discarding the ν value of the first 20-year slice that initializes the runoff simulation and reservoir operations, CRF of mean water scarcity was developed by a multiple regression between the remaining 499 ν values and the corresponding bi-decadal means of T_{avg} and P_{avg}. The logarithmic transformations were needed for normality of residuals. The variation of mean water scarcity could be explained by T_{avg} (°C) and P_{avg} (mm) with the following equation:

$$\log(\nu) = a + b \times \log(T_{avg}) + c \times \log(P_{avg}) + \in \tag{4}$$

where a, b, and c are regression coefficients, and ε is Gaussian noise that explain the randomness of ν, respectively.

Equation (4) allows linking directly between mean water scarcity and climatic conditions. For comparative assessment, we developed CRFs for three modeling cases by changing the storage capacity of the reservoir. The applied storage capacities were 0 Mm^3 (no reservoir), 2.3 Mm^3 (before upsizing), and 3.3 Mm^3 (after upsizing).

3.7. Downscaling GCMs

A total of 26 daily GCMs were collected from the archive of the Coupled Model Intercomparison Project Phase 5 (Taylor et al., 2012) to assess water scarcity under global warming for 2020–2099 (Table 1). The projections of daily precipitation and temperature were

Table 1
List of the GCMs for climate change impact assessments.

No.	Name of GCM	Resolution (Lat° × Lon°)	Institution
1	CMCC-CM	0.750 × 0.748	Centro Euro-Mediterraneo per I Cambiamenti Climatici
2	CMCC-CMS	1.875 × 1.865	
3	CCSM4	1.250 × 0.942	National Center for Atmospheric Research
4	CESM1-BGC	1.250 × 0.942	
5	CESM1-CAM5	1.250 × 0.942	
6	MRI-CGCM3	1.125 × 1.122	Meteorological Research Institute
7	CNRM-CM5	1.406 × 1.401	Centre National de Recherches Meteorologiques
8	HadGEM2-AO	1.875 × 1.250	Met Office Hadley Centre
9	HadGEM2-CC	1.875 × 1.250	
10	HadGEM2-ES	1.875 × 1.250	
11	INM-CM4	2.000 × 1.500	Institute for Numerical Mathematics
12	IPSL-CM5A-MR	2.500 × 1.268	Institut Pierre-Simon Laplace
13	MPI-ESM-LR	1.875 × 1.865	Max Planck Institute for Meteorology (MPI-M)
14	MPI-ESM-MR	1.875 × 1.865	
15	FGOALS-s2	2.813 × 1.659	LASG, Institute of Atmospheric Physics, Chinese Academy of Sciences
16	NorESM1-M	2.500 × 1.895	Norwegian Climate Centre
17	GFDL-ESM2G	2.500 × 2.023	Geophysical Fluid Dynamics Laboratory
18	GFDL-ESM2M	2.500 × 2.023	
19	BCC-CSM1-1	2.813 × 2.791	Beijing Climate Center, China Meteorological Administration
20	BCC-CSM1-1-M	1.125 × 1.122	
21	IPSL-CM5A-LR	3.750 × 1.895	Institut Pierre-Simon Laplace
22	IPSL-CM5B-LR	3.750 × 1.895	
23	MIROC5	1.406 × 1.401	Atmosphere and Ocean Research Institute, National Institute for Environmental Studies, and Japan Agency for Marine-Earth Science
24	MIROC-ESM-CHEM	2.813 × 2.791	and Technology
25	MIROC-ESM	2.813 × 2.791	
26	CanESM2	2.813 × 2.791	Canadian Centre for Climate Modelling and Analysis

downloaded for the representative concentration pathways (RCP) of RCP4.5 and RCP8.5 (available at https://esgf-node.llnl.gov/search/cmip5/). The RCP4.5 and RCP8.5 have been commonly used as scenarios of the stabilized and increasing GHG concentrations, respectively (e.g., He and Zhou, 2015).

The daily projections of GCMs were bias-corrected using the quantile-delta mapping (QDM) that explicitly preserves GCM-driven relative and absolute changes in all quantiles (Cannon et al., 2015; Eum and Cannon, 2016). It is an advanced quantile mapping method not only to adjust the marginal distributions of raw GCMs towards those of observations but also to preserve GCM-driven climate signals especially changes in extreme events. Further details and discussion are found in Cannon et al. (2015) and Eum and Cannon (Eum and Cannon, 2016). The baseline period was 1976–2005 to downscale the GCMs to the study area, while the forecast period was 2006–2099. For the impact assessments, T_{avg} and P_{avg} of the bias-corrected GCMs were calculated for the bi-decadal time slices of 2020–2039, 2040–2059, 2060–2079, and 2080–2099.

4. Results and discussion

4.1. Mean water scarcity under stochastic climates

Fig. 3 illustrates temporal variations of monthly water supply, demand, and water scarcity simulated by the stochastic precipitation and temperatures for two bi-decadal periods with distinct climatological means. The reservoir storage significantly contributed to reducing water scarcity at the demand site. With no reservoir storage (Fig. 3a,d), natural water supply was often unable to satisfy the irrigation demand in the early planting season. As described earlier, the rainy season begins typically in late June, such that streamflow is high in summer. Occasional rainfall events during the dry season (October to May) insufficiently recharge the watershed, generating low streamflow in the early rice-planting season (late April to early June) when irrigation water demand is high. Fig. 3b shows that the reservoir with storage of 2.3 Mm^3 could nullify discrepancies between the natural water supply and demand under a favorable climate ($T_{avg} = 11.5$ °C, $P_{avg} = 1529$ mm). However, water scarcity was becoming more frequent and more severe with increasing T_{avg} and decreasing P_{avg}. In an unfavorable climate ($T_{avg} = 15.4$ °C, $P_{avg} = 1442$ mm), water scarcity continued for multiple months even during rainy seasons. Upsizing the

reservoir to 3.3 Mm^3 (Fig. 3c) could alleviate the severe water scarcity under the unfavorable climate.

One main driver of severe water scarcity was insufficient inflows under unfavorable climates. The runoff ratio (the total streamflow divided by total precipitation) decreased by 33% from the favorable to the unfavorable climates in Fig. 3, indicating that the reservoir inflows sensitive to changes in P_{avg} and T_{avg}, primarily due to the soil moisture status and significant ET loss in the watershed. On the other hand, the total water demand showed low variability in the two stochastic climates, since the transplanting water requirement and the environmental demand were nearly constant.

Fig. 4 displays the scatter plots between mean water scarcity and stochastic climates of T_{avg} and P_{avg} for three scenarios of the reservoir storage capacity. The results show that increasing reservoir capacity significantly contributed to reducing mean scarcity, while its effectiveness was becoming more sensitive to changing climate. All mean water scarcity values in Fig. 4a (zero storage capacity) were greater than the other cases, implying that rice production is unsustainable without reservoir storages. When upsizing the reservoir to 3.3 Mm^3 (Fig. 4c), the mean water scarcity became less than 0.1 for all the pairs of (P_{avg}, T_{avg}).

However, it is also clearly indicated that a larger reservoir capacity made system performance more responsive to climatic changes. With the largest capacity among the three cases, the highest sensitivity of the mean scarcity was produced to changes in T_{avg} and P_{avg}. The coefficients of determination of the CRFs were 0.45, 0.78, and 0.86 for capacities of 0 Mm^3, 2.3 Mm^3, and 3.3 Mm^3, respectively. This implies that the correlation between climatic means and mean water scarcity becomes stronger with increasing reservoir capacity. This is because the major factor affecting discrepancies between inflows and demand in the early planting stage is not the climatic means, but the intra-annual climatic seasonality. In other words, water demands in this watershed cannot be satisfied by unregulated natural flows. In Fig. 3a, with zero reservoir storage, severe water scarcity from April to June occurred irrespective of the climatic means. The reservoir storage can reduce or nullify the water scarcity from climatic seasonality unexplained by T_{avg} and P_{avg}. Thus, as the storage capacity increases, T_{avg} and P_{avg} could explain the more variation of mean water scarcity. Briefly, the system analysis indicates that increasing the reservoir capacity made reservoir performance more sensitive and more correlated to shifting climatic means.
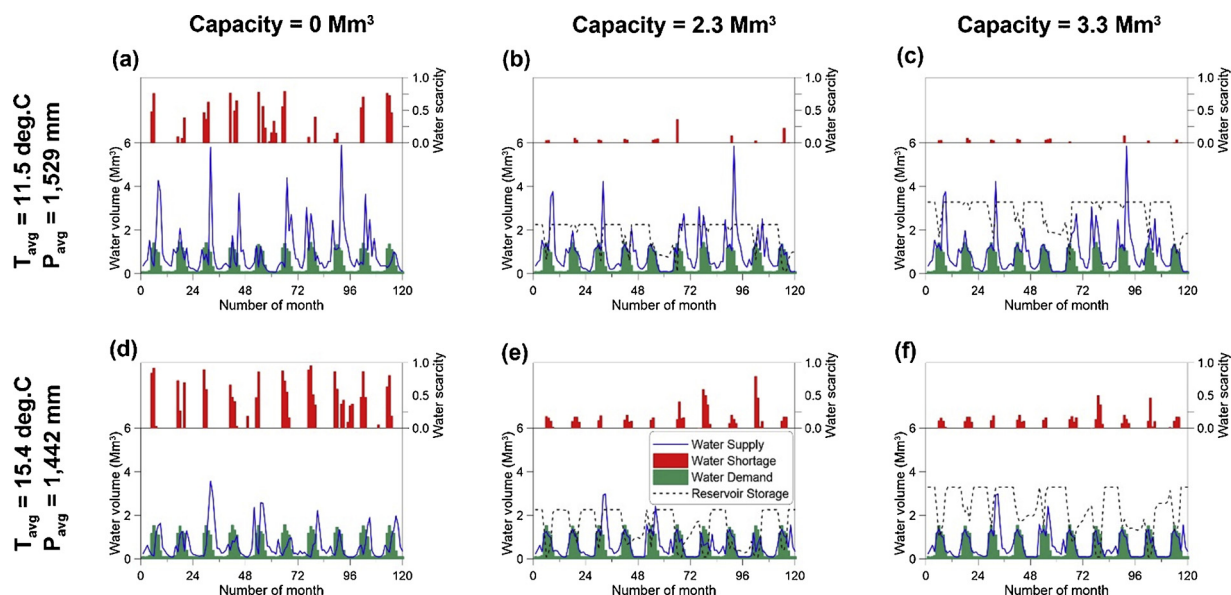

Fig. 3. The time series of water supply, demand, reservoir storage, and water scarcity under two distinct climatological means (a–c vs. d–f) under the three storage capacities of 0 Mm^3 (a,d), 2.2 Mm^3 (b,e), and 3.3 Mm^3 (c,f), respectively.
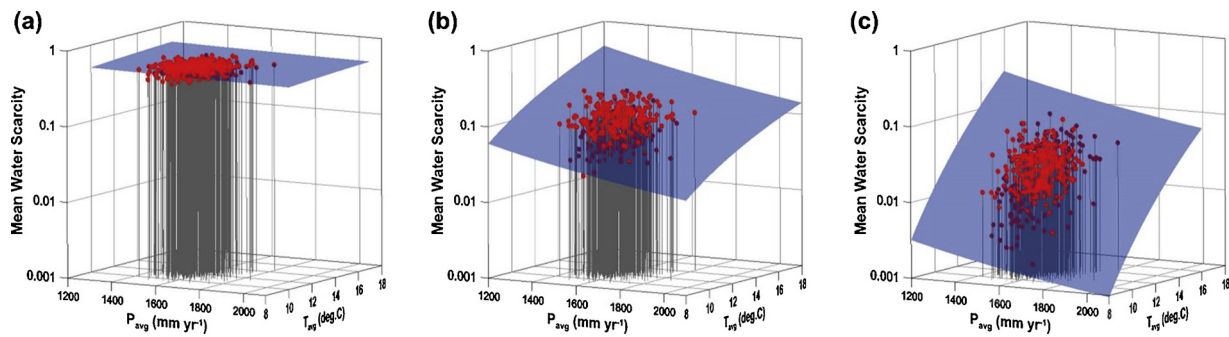
Fig. 4. Scatter plots of the mean water scarcity versus the stochastic bi-decadal averages of P_{avg} and T_{avg} (red dots), and CRFs developed by the multiple regressions (blue surfaces) for three reservoir capacities of (a) 0 Mm^3, (b) 2.2 Mm^3, and (c) 3.3 Mm^3, respectively. The p-values of the three regression models were less than 2.2×10^{-16}. (For interpretation of the references to colour in this figure legend, the reader is referred to the web version of this article.).
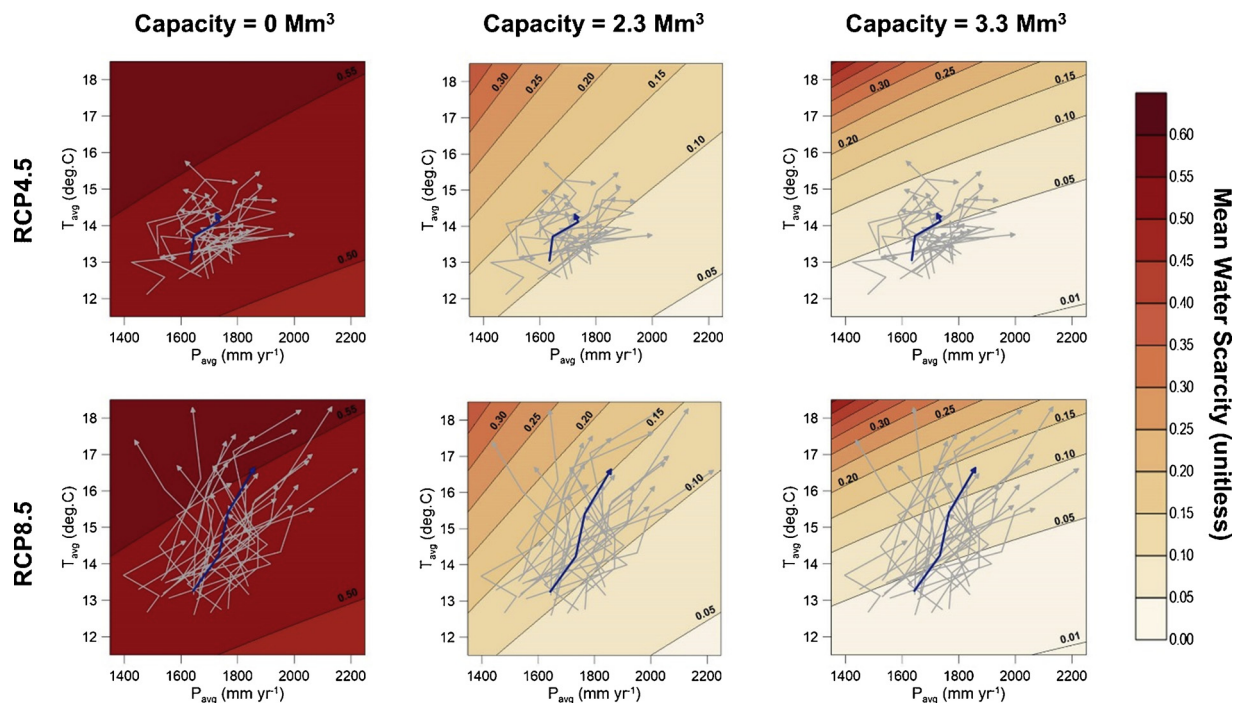

Fig. 5. Bi-decadal averages of P_{avg} and T_{avg} projected by 26 individual GCMs (gray) and their ensemble (navy blue) superimposed on CRFs of mean water scarcity for three reservoir capacities of 0 Mm^3 (left), 2.2 Mm^3 (middle), and 3.3 Mm^3 (right) under RCP4.5 (top) and RCP8.5 (bottom) scenarios. The straight lines connect four pairs of (P_{avg}, T_{avg}) for 2020–2039, 2040–2059, 2060–2079, and 2080–2099 projected by the GCMs indicating toward (P_{avg}, T_{avg}) for 2080–2099 (For interpretation of the references to colour in this figure legend, the reader is referred to the web version of this article.).

4.2. Assessing impacts of global warming on water scarcity

Fig. 5 presents the bias-corrected T_{avg} and P_{avg} projections by the 26 GCMs under RCP4.5 and RCP8.5 GHG emission scenarios. The four points of T_{avg} and P_{avg} for the bi-decadal time slices of 2020–2039, 2040–2059, 2060–2079, and 2080–2099 were connected by the continuous lines on the contoured CRFs. The GCM projections showed a large spread as expected from prior studies (e.g., Whateley et al., 2014; Orlowsky and Senevirantne, 2013). The large spread could be associated with cascade errors of GCM projections primarily induced from climate forcing (Stainforth et al., 2005), cloud feedbacks (Dufresne and Bony, 2008), initial conditions (Deser et al., 2012), and other insufficiently understood physical processes (New and Hulme, 2000), implying that deep uncertainties are present in GCM projections.

Despite sizeable incongruities between the GCMs, the ensemble of 26 models indicates that the study area may experience unprecedented severe water scarcity under both scenarios. It is worthy to focus on the contribution of temperature to water scarcity; higher T_{avg} produced higher mean water scarcity (refer to Fig. 5 for RCP 4.5 and RCP8.5 in

the case of capacity 3.3 Mm^3), mainly due to larger ET losses. Since the RCP4.5 scenario assumes stabilization of GHG concentration after 2050, changes in T_{avg} were expected to decrease with time. P_{avg} was expected to increase until 2060–2079 and slightly decrease in 2080–2099. Although individual GCMs provided a transition of T_{avg} with time, the ensemble projected continuously rising T_{avg} for the four time slices under the RCP 8.5 scenario hypothesizing increasing GHG concentration until 2100. On the other hand, the ensemble expected increasing P_{avg} under RCP8.5, while the individual projections were diverging. Based on the ensemble projections, the mean water scarcity was expected to be 0.07 and 0.13 for the case of 3.3 Mm^3 of reservoir capacity (i.e., after upsizing) under RCP4.5 and RCP 8.5 respectively. These are approximately 250% and 550% changes relative to 1996-2015. With 2.3 Mm^3 of reservoir capacity (i.e., before upsizing), the mean water scarcity would become 0.12 and 0.15 under RCP4.5 and RCP8.5, which are 33% and 67% changes relative to 1996-2015.

Fig. 5 highlights that the structural investment to the reservoir forced the system to be more responsive to shifting climatic means. Upsizing the reservoir seems more efficient when climatic changes are

less severe (i.e., RCP4.5). Under RCP8.5 scenario, the augmented capacity would minimally contribute to reducing the mean water scarcity during 2080–2099.

Nonetheless, it is noteworthy that the upsized reservoir system always provided the highest water supply performance among the three capacity scenarios. The system analysis already showed that the mean water scarcity with the expanded capacity was always less severe than the others. Upsizing the reservoir appears a paradoxical adaptation strategy. It improves water supply performance; however, the agricultural system was forced to be more responsive to climatic stresses.

4.3. Sensitivity of structural adaptations to climate change

By comparing between Fig. 5b and c, it is shown that system performance became more sensitive to rising temperatures than precipitation changes after upsizing the reservoir. This is because the additional capacity cannot reduce ET losses that occur across the watershed, while impacts of deficient precipitation can be minimized by extending the residence time of streamflow. Thus, as the reservoir capacity increases, increasing ET loss with rising temperatures would become a more significant factor to control system performance than decreasing precipitation.

A physical property explaining ET losses may explain the high sensitivity of increasing reservoir capacity to climate stresses. Fig. 6 presents a scatter plot between mean water scarcity and bi-decadal runoff ratio sampled by the stochastic performance tests. When climate becomes drier from high to low runoff ratios, mean water scarcity under the three storage scenarios appears to converge. This is the reason for the higher sensitivity of the system with a larger reservoir capacity. At an extremely dry climate, the reservoir becomes a run-of-river dam to supply water demands since the inflows are inadequate due to ET losses. In this case, there is no effectiveness from building or upsizing the reservoir, thus the mean water scarcity under the three modeling conditions should be the same. If climate alters towards extreme dryness, the improved performance gained from building or upsizing should rapidly decrease to converge to zero supply performance due to no surface water.

Fig. 7 conceptualizes the relationship between mean water scarcity and climate change. Under complete dryness with no surface water,
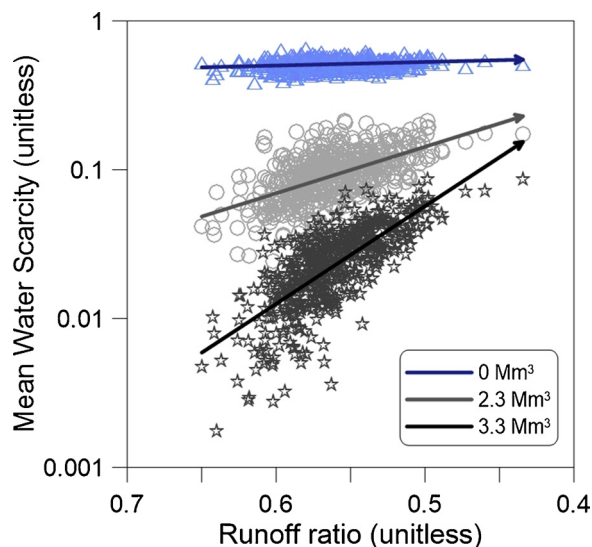

Fig. 7. Theoretical paths of mean water scarcity with no reservoir (A → A′), reservoir building (A → B → B′), and augmenting storage capacity (B → C → C′) when climate becomes drier.

mean water scarcity should become 100% (i.e., no water supply) regardless of storage capacity. While complete dryness is an unlikely scenario, the convergence determines the sensitivity of mean water scarcity to climate change. When a reservoir is constructed or upsized, mean water scarcity would decrease through the path of A→B or B→C. If climate is becoming drier, water scarcity would become severe through the path of B→B′ or C→C′. Importantly, the performance loss through the path of C→C′ is the highest among the three storage capacities. It should be noted that the relationship of water scarcity to runoff ration in Fig. 6 was non-linear. Hence, water scarcity could exponentially increase, if climate becomes drier.

Fig. 7 implies that managing the storage capacity could be an option to increase benefits from the system under a stationary climate rather than a "low regret" strategy for minimizing potential losses. The GCM projections driven by GHG emission scenarios have led to a controversial paradigm of 'dry gets drier, wet gets wetter' (Chou et al., 2013; Allan et al., 2010; Seager and Vecchi, 2010; Held and Soden, 2006; Liu and Allan, 2013; Greve et al., 2014). If this prediction is realized, building or upsizing reservoirs in dry regions may become a regretful decision. In a decision theory, humans tend to prefer avoiding losses to acquiring equivalent gains (Kahneman and Tversky, 1979). Managing the storage capacity in a drying environment may produce large potential regrets, if no soft measures (e.g., upgrading operations) are included.

4.4. Limitations

The focus of this study was the sensitivity of water supply performance to climatic changes in a simple reservoir system with no consideration of socioeconomic conditions. Thus, this work may appear to be counterintuitive to other studies conducted in larger and complex regions (e.g., Ehsani et al., 2017). Collective responses of many reservoirs to climatic stressors could differ from those of a small reservoir with a single demand sector. Since it always improves water supply performance, augmenting storage capacity can become a necessary adaptive measure for satisfying water demands.

In addition, the temperature-based PET model used in this study (Oudin et al., 2005) may overestimate the system sensitivity to rising temperatures. Several studies suggest that all four primary meteorological variables (i.e., radiation, air temperature, wind speed, and relative humidity) need to be considered for assessing long-term trends in ET, since declining rates of observed near-surface wind speed seem to be widespread across the globe (e.g., McVicar et al., 2012; Sheffield et al., 2012). While Oudin et al. (2005) proposed an efficient PET equation for lumped rainfall-runoff models, other PET models need to be tested for improving reliability of the CRFs.

Fig. 6. Relationships between mean water scarcity and the bi-decadal runoff ratio of the watershed for three reservoir capacities. The straight lines were regressed with exponential functions, indicating toward drier conditions. The blue, gray, and dark gray symbols are the 499 samples obtained from the stochastic system analyses (For interpretation of the references to colour in this figure legend, the reader is referred to the web version of this article.).
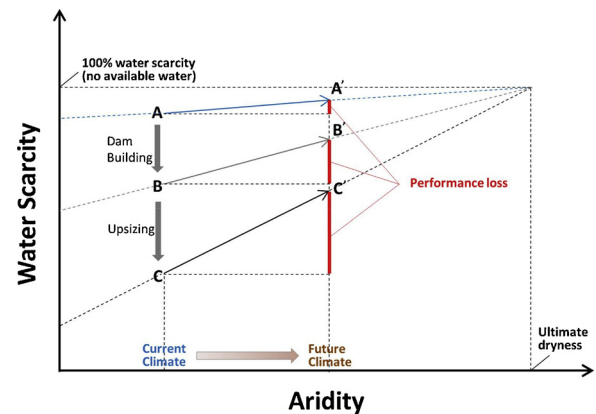
5. Conclusions

With growing concerns about the anthropogenic climate change and associated water scarcity risks, preparing appropriate adaptation strategies is of great importance especially for agriculture-dominated regions. In this paper, we showed that building or upsizing reservoirs make the system performance more sensitive to climatic stresses via a case study for a simple agricultural reservoir system. Upsizing the reservoir obviously provides effectiveness on reducing water scarcity. However, due to the high sensitivity to climatic stresses, it is expected to produce a minimal contribution in the study area for 2080–2099 under RCP8.5 scenario. A larger reservoir capacity should result in a more sensitive effectiveness to climate change since the system performance converges on zero impact under extreme dryness irrespective of reservoir capacity.

A key lesson from this study is that water supply performance of a small reservoir can exponentially decrease under a drying climate. As a consequence, potential losses in system performance could be much larger than before augmenting storage capacity. Therefore, it is worth emphasizing that the direction of climate change (i.e., drying or wetting) should be considered before applying a structural change for a simple reservoir system. It would also be necessary to formulate operational measures along with the structural changes for reducing sensitivity of the reservoir system to climatic stressors.

References

Adgar, W.N., Arnell, N.W., Tompkins, E.L., 2005. Successful adaptation to climate change across scales. Glob. Environ. Change 15, 77–86.

Allan, R.P., Soden, B.J., John, V.O., Ingram, W., Good, P., 2010. Current changes in tropical precipitation. Environ. Res. Lett. 5, 025205.

Allen, R.G., Pereira, L.S., Raes, D., Smith, M., 1998. Crop evapotranspiration: guidelines for computing crop water requirement. FAO Irrig. Drain., Paper No. 56. Food and Agr. Orgn. of the United Nations. Rome.

Bae, D.-H., Jung, I.-W., Chang, H., 2008. Long-term trend of precipitation and runoff in Korean river basins. Hydrol. Process. 22, 2644–2656.

Biemans, H., Haddeland, I., Kabat, P., Ludwig, F., Hutjes, R.W.A., Heinke, J., von Bloh, W., Gerten, D., 2011. Impact of reservoirs on river discharge and irrigation water supply during the 20th century. Water Resour. Res. 47https://doi.org/10.1029/2009WR008929. W03509.

Brown, C., Wilby, R.L., 2012. An alternate approach to assessing climate risks. Eos Trans. AGU 93 (41), 401.

Brown, C., Ghile, Y., Laverty, M., Li, K., 2012. Decision scaling: linking bottom-up vulnerability analysis with climate projections in the water sector. Water Resour. Res. 48 (9). https://doi.org/10.1029/2011WR011212. W09537.

Cannon, A.J., Sobie, S.R., Murdock, T.Q., 2015. Bias correction of GCM precipitation by quantile mapping: How well do methods preserve changes in quantiles and extremes? J. Clim. 28, 6938–6959.

Cho, J., Ko, G., Kim, K., Oh, C., 2016. Climate change impacts on agricultural drought with consideration of uncertainty in CMIP5 Scenarios. Irrig. Drain. 65, 7–15. https://doi.org/10.1002/ird.2035.

Chou, C., Chiang, J.C.H., Lan, C.-W., Chung, C.-H., Liao, Y.-C., Lee, C.-J., 2013. Increase in the range between wet and dry season precipitation. Nat. Geosci. 6, 263–267.

Daly, C., Halbleib, M., Smith, J.I., Gibson, W.P., Doggett, M.K., Taylor, G.H., Curtis, J., Pasteris, P.P., 2008. Physiographically sensitive mapping of climatological temperature and precipitation across the conterminous United States. Int. J. Climatol. 28, 2031–2064. https://doi.org/10.1002/joc.1688.

Deser, C., Phillips, A., Bourdette, V., Teng, H., 2012. Uncertainty in climate change projections: the role of internal variability. Clim. Dyn. 38, 527–546. https://doi.org/10.1007/s00382-010-0977-x.

Downing, J.A., Prairie, Y.T., Cole, J.J., Duarte, C.M., Tranvik, L.J., Striegl, R.G., McDowell, W.H., Kortelainen, P., Caraco, N.F., Melack, J.M., Middelburg, J.J., 2006. The global abundance and size distribution of lakes, ponds, and impondments. Limnol. Oceanogr. 51 (5). https://doi.org/10.4319/lo.2006.51.5.2388.

Dufresne, J.-L., Bony, S., 2008. An assessment of the primary sources of spread of global warming estimates from coupled atmosphere-ocean models. J. Clim. 21, 5135–5144.

Ehsani, N., Vörösmarty, C.J., Fekete, B.M., Stakhiv, E.Z., 2017. Reservoir operations under climate change: storage capacity options to mitigate risk. J. Hydrol. 555, 435–446.

Eum, H.-I., 2015. High-resolution gridded data generation and performance assessment of multiple statistical downscaling methods for South Korea. APEC Climate Center Research Report 2015-05.

Eum, H.-I., Cannon, A.J., 2016. Intercomparison of projected changes in climate extremes for South Korea: application of trend preserving statistical downscaling methods to the CMIP5 ensemble. Int. J. Climatol. 37 (8), 3381–3397. https://doi.org/10.1002/joc.

Eum, H.-I., Simonovic, S.P., 2010. Integrated reservoir management system for adaptation to climate change: the Nakdong River basin in Korea. Water Resour. Manage. 24, 3397–3417. https://doi.org/10.1007/s11269-010-9612-1.

Eum, H.-I., Kim, Y.-O., Palmer, R.N., 2011. Optimal drought management using sampling stochastic dynamic programming with a hedging rule. J. Water Res. Plan. Manag. 137 (1), 113–122.

Georgakakos, A.P., Yao, H., Kistenmacher, M., Georgakakos, K.P., Graham, N.E., Cheng, F.-Y., Spencer, C., Shamir, E., 2012. Value of adaptive water resources management in Northern California under climatic variability and change: reservoir management. J. Hydrol. 412-413, 34–46. https://doi.org/10.1016/j.jhydrol.2011.04.038.

Greve, P., Orlowsky, B., Mueller, B., Sheffield, J., Reichstein, M., Seneviratne Sonia, I., 2014. Global assessment of trends in wetting and drying over land. Nat. Geosci. 7, 716–721. https://doi.org/10.1038/NGEO2247.

Hallegatte, S., 2009. Strategies to adapt to an uncertain climate change. Glob. Environ. Chang. 19, 240–247. https://doi.org/10.1016/j.gloenvcha.2008.12.003.

Hashimoto, T., Stedinger, J.R., Loucks, D.P., 1982. Reliability, resiliency, and vulnerability criteria for water resource system performance evaluation. Water Resour. Res. 18, 14–20.

He, C., Zhou, T., 2015. Responses of the western North Pacific Subtropical High to global warming under RCP4.5 and RCP8.5 scenarios projected by 33 CMIP5 models: the dominance of tropical Indian Ocean–tropical western Pacific SST gradient. J. Clim. 28, 365–380.

Held, I.M., Soden, B.J., 2006. Robust responses of the hydrological cycle to global warming. J. Clim. 19, 5686–5699.

Iglesias, A., Garrote, L., 2015. Adaptation strategies for agricultural water management under climate change in Europe. Agric. Water Manage. 155, 113–124. https://doi.org/10.1016/jagwat.2015.03.014.

IPCC, 2007. In: Core Writing Team, Pachauri, R.K., Reisinger, A. (Eds.), Climate Change 2007: Synthesis Report. Contribution of Working Groups I, II and III to the Fourth Assessment Report of the Intergovernmental Panel on Climate Change. IPCC, Geneva, Switzerland, pp. 104.

Jung, Y., Eum, H.-I., 2015. Application of a statistical interpolation method to correct extreme values in high-resolution gridded climate variables. J. Clim. Change Res. 6, 331–334.

Kahneman, D., Tversky, A., 1979. An analysis of decision under risk. Econometrica 47, 263–291.

Keller, D.E., Fischer, A.M., Frei, C., Liniger, M.A., Appenzeller, C., Knutti, R., 2015. Implementation and validation of a Wilks-type multi-site daily precipitation generator over a typical Alpine river catchment. Hydrol. Earth Syst. Sci. 19, 2163–2177.

Khagram, S., 2004. Dams and Development: Transitional Struggles for Water and Power. First Cornell University Press, Ithaca, USA.

Kim, D., Jung, I.W., Chun, J.A., 2017. A comparative assessment of rainfall–runoff modelling against regional flow duration curves for ungauged catchments. Hydrol. Earth Syst. Sci. 21, 5647–5661. https://doi.org/10.5194/hess-21-5647-2017.

Li, Q., Gowing, J., 2005. A daily water balance model approach for simulating performance of tank-based irrigation systems. Water Resour. Manage 19, 211–231.

Liu, C., Allan, R.P., 2013. Observed and simulated precipitation responses in wet and dry regions 1850–2100. Environ. Res. Lett. 8, 034002.

Loucks, D.P., van Beek, E., 2016. Water Resource Systems Planning and Management. An Introduction to Methods, Models, and Applications. Springer Nature, Gewerbestrasse, Switzerland.

Maass, A., Hufschmidt, M.M., Dorfman, R., Thomas, H.A., Marglin, S.A., Fair, G.M., 1962. Design of Water-Resource Systems. Harvard Univ. Press, Cambridge, Massachusetts, USA.

McVicar, T.R., Roderick, M.L., Donohue, R.J., Li, L.T., Van Niel, T.G., Thomas, A., Grieser, J., Jhajharia, D., Himri, Y., Mahowald, N.M., Mescherskaya, A.V., Kruger, A.C., Rehman, S., Dinpashoh, Y., 2012. Global review and synthesis of trends in observed terrestrial near-surface wind speeds: implications for evaporation. J. Hydrol. 416-417, 182–205.

New, M., Hulme, M., 2000. Representing uncertainty in climate change scenarios: a Monte-Carlo approach. Integr. Assess. 1, 203–213.

Ngigi, S.N., 2003. What is the limit of up-scaling rainwater harvesting in a river basin? Phys. Chem. Earth 28, 943–956.

Nilsson, C., Reidy, C.A., Dynesius, M., Revenga, C., 2005. Fragmentation and flow regulation of the world's large river systems. Science 308, 405–408.

Orlowsky, B., Seneviratne, S.I., 2013. Elusive drought: uncertainty in observed trends and short- and long-term CMIP5 projections. Hydrol. Earth Syst. Sci. 17, 1765–1781. https://doi.org/10.5194/hess-17-1765-2013.

Oudin, L., Hervieu, F., Michel, C., Perrin, C., Andréassian, V., Anctil, F., Loumagne, C., 2005. Which potential evapotranspiration input for a lumped rainfall–runoff model?: part 2—towards a simple and efficient potential evapotranspiration model for rainfall–runoff modelling. J. Hydrol. 303, 290–306.

Perrin, C., Michel, C., Andréassian, V., 2003. Improvement of a parsimonious model for streamflow simulation. J. Hydrol. 279, 275–289.

Poff, N.L., Olden, J.D., 2017. Can dams be designed for sustainability? Science 358, 1252–1253. https://doi.org/10.1126/science.aaq1422s.

Poff, N.L., Schmidt, J.C., 2016. How dams can go with the flow. Small changes to water flow regimes from dams can help to restore river ecosystems. Science 353, 1099–1100. https://doi.org/10.1126/science.aah4926.

Raje, D., Mujumdar, P.P., 2010. Reservoir performance under uncertainty in hydrologic impacts of climate change. Adv. Water Resour. 33, 312–326.

Seager, R., Vecchi, G.A., 2010. Greenhouse warming and the 21st century hydroclimate of southwestern North America. Proc. Natl. Acad. Sci. U. S. A. 107, 21277–21282.

Sheffield, J., Wood, E.F., Roderick, M.L., 2012. Little change in global drought over the past 60 years. Nature 491, 435–438. https://doi.org/10.1038/nature11575.

Srikanthan, R., Pegram, G.G., 2009. A nested multisite daily rainfall stochastic generation model. J. Hydrol. 371, 142–153.

Stainforth, D.A., Aina, T., Christensen, C., Collins, M., Faull, N., Frame, D.J., Kettleborough, J.A., Knight, S., Martin, A., Murphy, J.M., Piani, C., Sexton, D., Smith, L.A., Spicer, R.A., Thorpe, A.J., Allen, M.R., 2005. Uncertainty in predictions of the climate response to rising levels of greenhouse gases. Nature 433, 403–406.

Stedinger, J.R., 1984. The performance of LDR models for preliminary design and reservoir operation. Water Resour. Res. 14, 984–986.

Steinschneider, S., Brown, C., 2012. Dynamic reservoir management with real-option risk hedging as a robust adaptation to nonstationary climate. Water Resour. Res. 48, W11525. https://doi.org/10.1029/2011WR011318.

Steinschneider, S., McCrary, R., Wi, S., Mulligan, K., Mearns, L.O., Brown, C., 2015. Expanded decision-scaling framework to select robust long-term water-system plans under hydroclimatic uncertainties. J. Water Resour. Plann. Manage. 141 04015023-1.

Taylor, K.E., Stouffer, R.J., Meehl, G.A., 2012. An overview of CMIP5 and the experiment design. Bull. Am. Meteorol. Soc. 93, 485–498.

Turner, S.W.D., Marlow, D., Ekström, M., Rhodes, B.G., Kularathna, U., Jeffrey, P.J., 2014. Linking climate projections to performance: a yield-based decision scaling assessment of a large urban water resources system. Water Resour. Res. 50, 3553–3567. https://doi.org/10.1002/2013WR015156.

Vano, J.A., Scott, M.J., Voisin, N., Stöckle, C.O., Hamlet, A.F., Mickelson, K.E.B., Elsner, M.M., Lettenmaier, D.P., 2010. Climate change impacts on water management and irrigated agriculture in the Yakima river basin, Washington, USA. Clim. Change 102, 287–317.

Weaver, C.P., Lempert, R.J., Brown, C., Hall, J.A., Revell, D., Sarewitz, D., 2013. Improving the contribution of climate model information to decision making: the value and demands of robust decision frameworks. WIREs Clim. Change 4, 39–60. https://doi.org/10.1002/wcc.202.

Whateley, S., Steinschneider, S., Brown, C., 2014. A climate change range-based method for estimating robustness for water resources supply. Water Resour. Res. 50, 8944–8961. https://doi.org/10.1002/WR015956.

Wilby, R.L., Dessai, S., 2010. Robust adaptation to climate change. Weather 65, 180–185. https://doi.org/10.1002/wea.543.

Wilks, D.S., 1999. Simultaneous stochastic simulation of daily precipitation, temperature and solar radiation at multiple sites in complex terrain. Agric. For. Meteorol. 96, 85–101.

Wisser, D., Frolking, S., Douglas, E.M., Fekete, B.M., Schumann, A.H., Vörömarty, C.J., 2010. The significance of local water resources captured in small reservoir for crop production. J. Hydrol. 384, 264–275.

Yoo, S.-H., Choi, J.-Y., Jang, M.-W., 2006. Estimation of paddy rice crop coefficients for FAO Penman-Monteith and modified Penman method. J. Korean Soc. Agric. Eng. 48, 13–23 written in Korean.

Zhang, Y., Vaze, J., Chiew, F.H.S., Li, M., 2015. Comparing flow duration curve and rainfall-runoff modelling for predicting daily runoff in ungauged catchments. J. Hydrol. 525, 72–86.